Ab Initio GW Many-Body Effects in Graphene

Paolo E. Trevisanutto,[1,2] Christine Giorgetti,[3,2] Lucia Reining,[3,2] Massimo Ladisa,[4] and Valerio Olevano[1,2]

[1]*Institut Néel, CNRS and UJF, Grenoble, France*
[2]*European Theoretical Spectroscopy Facility (ETSF), Paris, France*
[3]*Laboratoire des Solides Irradiés, CNRS-CEA, École Polytechnique, Palaiseau, France*
[4]*Istituto di Cristallografia, CNR, Bari, Italy*
(Received 28 March 2008; published 26 November 2008)

We present an *ab initio* numerical many-body *GW* calculation of the band plot in freestanding graphene. We consider the full ionic and electronic structure introducing *e-e* interaction and correlation effects via a self-energy containing non-Hermitian and dynamical terms. With respect to the density-functional theory local-density approximation, the Fermi velocity is renormalized with an increase of 17%, in better agreement with the experiment. Close to the Dirac point the linear dispersion is modified by the presence of a kink, as observed by angle-resolved photoemission spectroscopy. We demonstrate that the kink is due to low-energy $\pi \rightarrow \pi^*$ single-particle excitations and to the π plasmon. The *GW* self-energy does not open the band gap.

The discovery of graphene by micromechanical cleavage [1,2] and epitaxial grow [3] has attracted tremendous interest in consideration of its unusual electronic properties. In the tight-binding formalism, the graphene 2D honeycomb lattice structure gives rise to a semiconductor with zero band gap occurring at the K point in the Brillouin zone and a conelike linear band dispersion at low energy. This part is usually described by a massless Dirac (Weyl) dispersion [4]. *Ab initio* density-functional theory (DFT) calculations [5] confirm the tight-binding linear dispersion picture and give an estimate of the Fermi velocity v_F lower by 15%–20% than the experimental value. Recently, two angle-resolved photoemission spectroscopy (ARPES) experiments on graphene epitaxially grown on SiC [6–10] raised the general interest. The first one [6,9] observed at low energy a nearly linear band dispersion with slight deviations in the form of small kinks interpreted as due to many-body electron-electron (*e-e*) and electron-phonon (*e*-ph) self-energy effects. The second one [7,8,10] provided a different picture, with the opening of a band gap occurring at the Dirac K point and attributed either to substrate (SiC) or to many-body self-energy effects. A DFT calculation [11] seemed to confirm a substrate induced symmetry breaking, but recent STM measures [12] provided some evidence to exclude it. This situation calls for clarification about the role of *e-e* self-energy effects on the quasiparticle (QP) band plot, the Fermi velocity, and the band gap opening. Previous *ab initio* works have dealt with *e*-ph effects [5,13] and with *e-e GW* effects in graphene nanoribbons [14]. There are also several *non-ab initio* works [15–18] which studied *e-e* self-energy effects in a 2D massless Dirac model.

In this work we calculate the band plot of freestanding undoped graphene introducing *e-e* interaction and correlation effects by an *ab initio* many-body *GW* self-energy [19,20]. We numerically simulate the full ionic and elec-

tronic structure of real graphene. We take into account the full dynamical dependence and non-Hermiticity of the self-energy by an accurate contour-deformation (CD) integration. From the self-energy we then obtain the QP energies and the spectral function which can be directly compared with ARPES spectra. We show that the *GW* self-energy renormalizes the Fermi velocity by 17% such that it corrects the DFT underestimation and leads to a value of 1.12×10^6 ms^{-1}, in good agreement with the accurate magnetotransport measure of 1.1×10^6 ms^{-1} [2]. Furthermore, the nearly linear DFT band dispersion is in *GW* considerably distorted. Close to the Dirac point the self-energy results in an unusual negative *GW* band gap correction and the appearance of a kink in the band plot, leading to a scenario similar to that observed in ARPES; Ref. [6]. A comparison with the results of a *GW* plasmon-pole model calculation indicates that the kink is due to a coupling with the π plasmon at ~5 eV and the low-energy $\pi \rightarrow \pi^*$ single-particle excitations (SPE) shoulder present in the energy-loss function. This provides a partial confirmation to the explanation given in Ref. [6]. Finally, our results show that in freestanding graphene the *GW* self-energy does not open the band gap, in contrast to what is found in *GW* calculations on graphene nanoribbons [14].

Our starting point is a standard ground-state DFT local-density approximation (LDA) calculation of infinite freestanding graphene. We use a plane waves basis set (62 Ry cutoff) and periodic boundary conditions on a hexagonal cell containing 2 carbon atoms ($a = 2.4$ Å) and 38 bohr of vacuum along the z direction, large enough to isolate spurious replica of graphene sheets. We use Martins-Trouiller norm-conserving pseudopotentials with s and p electrons in the valence. We first calculate the ground-state energy and electronic density, and then the Kohn-Sham (KS) electronic structure to be used as the starting point in the following *GW* excited-state calculation.

In the *GW* approximation [19,20] the self-energy is

$$\Sigma^{GW}(r, r', \omega) = \frac{i}{2\pi} \int_{-\infty}^{\infty} d\omega' G(r, r', \omega - \omega') W(r, r', \omega'),$$

that is the product of Green's function G and the dynamically screened interaction $W(\omega) = \varepsilon^{-1}(\omega)v$ defined as the bare Coulombian interaction v screened by the dynamical dielectric function $\varepsilon^{-1}(\omega)$. Vertex corrections are neglected both in the self-energy and in the polarizability (hence in W). In the standard *ab initio GW* resolution procedure one builds G and W using the DFT KS electronic structure. The integral over the frequency is performed by a CD method [21] which consists in a deformation of the real axis contour such as to calculate the self-energy as an integral along the imaginary axis minus a contribution arising from the residual of the contour-included poles of G. This is the most accurate method to perform a *GW* calculation. We also considered the standard *plasmon-pole* model (PPM) approach [20]. Once the integration is performed, we calculate the *GW* quasiparticle energies using a first-order perturbation theory expansion of Σ around the LDA exchange-correlation potential v_{xc}^{LDA} and the KS energies $\omega = \epsilon_{nk}^{KS}$,

$$\epsilon_{nk}^{GW} = \epsilon_{nk}^{KS} + Z\langle nk | \Sigma^{GW}(\omega = \epsilon_{nk}^{KS}) - v_{xc}^{LDA} | nk \rangle,$$

where $Z = (1 - \partial\Sigma^{GW}/\partial\omega|_{\omega=\epsilon_{nk}^{KS}})^{-1}$ is the renormalization factor. We compare these energies to the positions of QP peaks in the spectral function

$$A_n(k, \omega) = \frac{\pi^{-1} |\operatorname{Im}\Sigma_n(k, \omega)|}{[\omega - \epsilon_{nk}^{KS} + v_{nk}^{xc} - \operatorname{Re}\Sigma_n(k, \omega)]^2 + [\operatorname{Im}\Sigma_n]^2}$$

calculated at the given k point in the Brillouin zone and projected on the considered n band.

We used the ABINIT code. Convergence was achieved with 715 plane waves (10 Ry) to represent the wave functions and the exchange part Σ_x of the self-energy, 150 and 200 bands to calculate respectively W and Σ [22]. The dimension of W and of the correlation part Σ_c as reciprocal space matrices was 169 (6 Ry). Imaginary axis integrations were carried out by a Gauss quadrature using 10 nodes for the most accurate calculations and W was sampled every 0.2 eV over 100 frequencies on the real axis. The Brillouin zone was sampled with a (10 10 1) Monkhorst-Pack k-point grid.

In Fig. 1 we compare the KS DFT-LDA (thick lines) and the quasiparticle *GW* (circles and dashed lines) electronic structures. Exchange end correlations effects slightly affect the band shapes. Relevant effects are a lowering of the σ bands and an increase (up to +20%) of the gaps at M (4 → 4.8 eV) and at Γ (6.4 → 7 eV). This is a normal behavior of *GW* and in agreement with other calculations [23,24]. We now focus on the Fermi energy Dirac point (K) region (Fig. 2). As previously obtained [5], the DFT KS π and π^* (thick lines) band dispersion is linear in the first ~0.5 Å^{-1} from the Dirac K point. The DFT KS Fermi velocity is 0.95×10^6 ms^{-1}. This underestimates by 15% the experi-
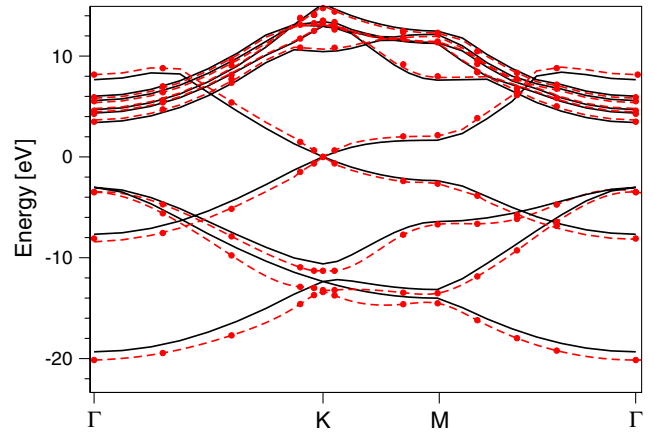

FIG. 1 (color online).   Band plot of graphene. Solid thick lines: DFT-LDA KS; circles and dashed lines: *GW*.

mental value. The dots and thin lines represent the *GW* band plot calculated by the CD method. The first evident self-energy effect is the loss of linearity along the region 0.05 Å^{-1} close to the Dirac K point. However, outside that region the linearity is soon recovered but with a slope larger than the DFT KS. A fit of the *GW* band with a straight line (dashed line) gives a Fermi velocity of 1.12×10^6 ms^{-1} (1.14 with $a_{th} = 2.45$ Å). Thus the *GW* self-energy *renormalizes* by +17% the DFT Fermi velocity and achieves a good agreement with the experimental measure of 1.1×10^6 ms^{-1} [2]. The residual overestima-
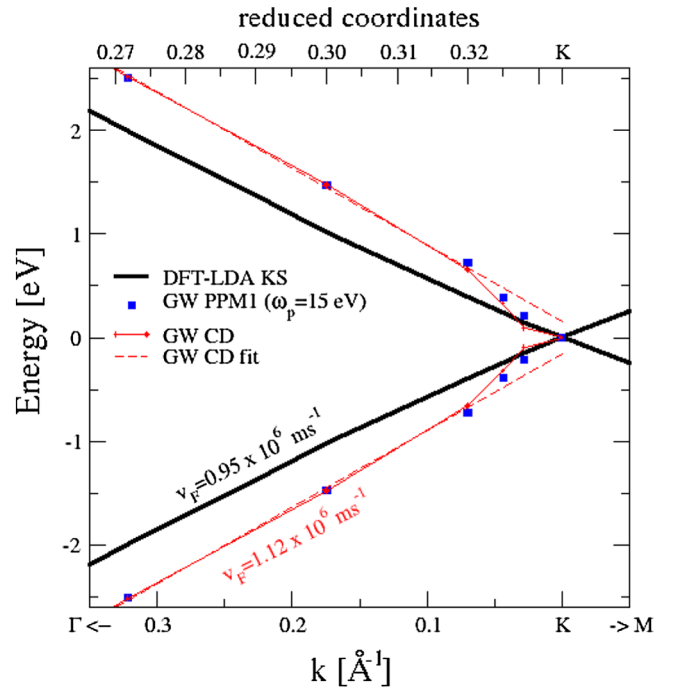

FIG. 2 (color online).   Focus on the band plot Dirac point region. Solid thick line: DFT-LDA KS; circles and thin lines: *GW* CD; squares: *GW* PPM1 ($\omega_p \simeq 15$ eV); dashed line: fit over the *GW* CD linear region.

tion of 2%–4% should be compensated by negative *e*-ph renormalization effects (−4% in Ref. [13]).

We now focus on the nonlinear region. In all the *k* points far from the Dirac point, the *GW* correction acts in the usual direction to open the gap between DFT KS bands. On the other hand, at $k = (0.328, 0.328, 0)$ (reduced coordinates), that is at ~ 0.025 Å^{-1} from *K*, we have found an unusual *negative GW correction* of −0.12 eV [25] which generates a *kink* at ~ 0.1 eV from the Dirac point. This result reproduces the experimental ARPES scenario of Ref. [6] where a kink interpreted as due to *e-e* many-body effects is found more or less in this position. The position of our *GW* kink is also close to the position indicated in the other ARPES experiment [gray arrows in Fig. 3(d) of Ref. [8] at 0.035 Å^{-1} and 0.17 eV].

The negative *GW* correction conjuring the kink results from an unusual balance between the exchange and the correlation energy (see Table I). Indeed, the exchange energy difference between the bottom of conduction band 5 and the top of valence band 4, $\langle \Delta \Sigma_x \rangle$, is typically several times larger than the difference in the correlation energy $\langle \Delta \Sigma_c \rangle$ which opposes the exchange energy [19,20]. At the kink $\Delta \Sigma_c$ is $\simeq 0.7$ eV, larger than $\Delta \Sigma_x \simeq 0.5$ eV. Therefore the negative correction to the band gap is due to a correlation energy stronger than usual. We report in Fig. 2 and Table I the result obtained by a PPM *GW* calculation (indicated as PPM1 and squares). Far from the Dirac point and exactly at the Dirac point (where the gap correction vanishes), the PPM *GW* bands precisely recover the CD result. PPM and CD start to deviate in the kink region, and at the kink point the PPM provides, in contrast to CD, a positive *GW* correction. This has an immediate interpretation. In the PPM approach the dynamical dependence of the energy-loss function $-\mathrm{Im}\,\varepsilon^{-1}$ entering into *W* and the *GW* self-energy is represented by a single plasmon-pole feature which is fitted to $\mathrm{Re}\,\varepsilon^{-1} = 1 + \Omega^2/(\omega^2 - \omega_p^2)$. This is a good approximation in all systems where the energy-loss function presents a single plasmon feature. In graphene the energy-loss function $-\mathrm{Im}\,\varepsilon^{-1}(q \simeq 0, \omega)$, as calculated from first-principles by the DP code in the RPA approximation (solid line in Fig. 3), shows two major features: the total $\pi + \sigma$ plasmon at ~ 15 eV and the π plasmon at ~ 5 eV [see Fig. 1(e) of Refs. [26,27]]. Furthermore, at the lowest energies there is a shoulder due to the $\pi \rightarrow \pi^*$ SPE. In our PPM1 *GW* calculation,

the plasmon-pole frequency at $q \simeq 0$ sets to $\omega_p = 15$ eV (dot-dashed arrow) at the left side of the total plasmon peak. It reproduces the main energy-loss feature and implicitly accounts also for the low-energy part of the spectrum. Other PPM calculations are examined (PPM2 in Fig. 3 and Table I). Forcing the plasmon pole to adjust to $\omega_p \simeq 5$ eV, the low-energy part of the energy loss is explicitly considered. In this case the resulting *GW* correction is around 0, closer to the correct *GW* CD result. Finally, we performed a CD calculation where ε^{-1} is computed cutting off low-energy $\pi \rightarrow \pi^*$ SPE (2.5 eV IR cutoff). The low-energy shoulder is suppressed (dotted line in Fig. 3) and the intensity of the π plasmon is also unavoidably reduced. The IR cutoff has the effect of producing a positive *GW* correction even beyond the PPM1 result, thus validating the good quality of the PPM. From all these results we can deduce that both the π plasmon and the low-energy $\pi \rightarrow \pi^*$ SPE shoulder provide the crucial contribution to the correlation energy and play a major role in conjuring the negative *GW* correction and the kink.

The last important result of our *GW* calculation is that many-body effects, within the numerical error bar, do not open the band gap at the Dirac point. Both the CD and the PPM do not change the DFT-LDA 0 band gap and bands 4 and 5 keep degenerate at *K* [28]. We find no indication for a band gap opening even when looking at the spectral function. In Fig. 4 we reported the real (bottom panel) and the module of the imaginary part (middle) of the self-energy at the Dirac *K* point projected onto bands 4 (solid line) and 5 (dashed line). The intersection of the real part of $\Sigma_{nk}(\omega)$ with the straight line $\omega - \epsilon_{nk}^{KS} + \upsilon_{nk}^{xc}$ gives the position of the QP peak. Although $\mathrm{Re}\,\Sigma$ is different for bands 4 and 5, the intersections occur at the same point, so that the QP peaks are degenerate. The correspondent $\mathrm{Im}\,\Sigma$ is in practice numerically 0. In the spectral function (top panel) we observe well-defined QP peaks and weak π and $\pi + \sigma$ plasmon satellites pointing to a normal Fermi liquid, unlike
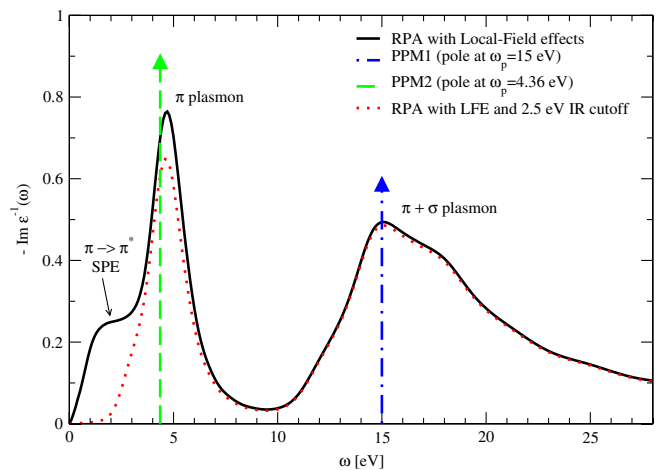
TABLE I. Exchange and correlation component differences between bands 5 and 4, renormalization factor *Z*, and *GW* band gap opening (energies in eV; *Z* as pure numbers).

k	Method	$-\Delta \upsilon_{xc}^{\mathrm{LDA}}$	$\Delta \Sigma_x$	$\Delta \Sigma_c^{GW}$	*Z*	$\Delta \epsilon^{GW}$
K	CD	−0.023	0.032	−0.008	0.729	+0.001
0.328	CD	−0.011	0.493	−0.689	$\simeq 0.71$	−0.121
0.328	PPM1	−0.011	0.493	−0.316	$\simeq 0.76$	+0.127
0.328	PPM2	−0.011	0.493	−0.453	0.537	+0.016
0.328	CD IR cut	−0.011	0.493	−0.273	0.771	+0.162

FIG. 3 (color online).   Graphene energy-loss function at $q \simeq 0$. Solid line: RPA with local-field effects (LFE); arrows: positions of the PPM1 (dot-dashed line) and PPM2 (dashed line) poles.
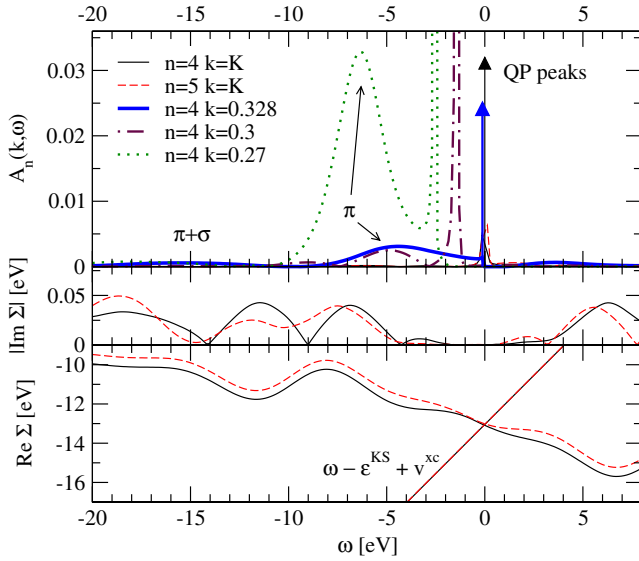
FIG. 4 (color online).   Graphene real and imaginary part of the self-energy and spectral function projected on bands 4 and 5 and at several k points.

Refs. [15–18]. Thus our calculation excludes a band gap opening, even only apparent [18], induced by a consistent transfer of weight from QP peaks to strong satellite plasmarons [16].

Finally, we want to discuss possible mechanisms which can explain the presented picture. A simple kink, i.e., a slope change of the bands in one point, has been obtained in Ref. [29] by invoking a purely dynamical, k-independent, mechanism; this model is most adequate for strongly correlated systems like some transition metal oxides. The situation in graphene, with its negative GW correction and consequent s-shaped kink, requires a more complex description. We can indeed understand the results by using a simplified PPM which accounts only for the low lying $\pi \to \pi^*$ SPE and the π plasmon. It has been shown [27] that for this plasmon we can assume a linear dispersion $\omega_p(q) = \omega_p^0 + \alpha q$ with a finite $\omega_p^0 \neq 0$. Together with other straightforward assumptions, this model leads to a correlation energy in the form

$$\Sigma_c^{GW} \simeq \frac{\Omega^2}{v_F \omega_p^0}[\log((v_F + \alpha)k + \omega_p^0) - \log(\alpha k + \omega_p^0)],$$

which in the limit $k \to \infty$ tends to a constant whereas in the limit $k \to k_F$ is linear like the exchange energy $\Sigma_x \sim k$, but with a coefficient $\Omega^2/2\omega_p^{02}$ times the exchange. This hypothesis is compatible with a zero band gap at $k = k_F$ and yields a large-k region where the exchange dominates and renormalizes the Fermi velocity. If $\Omega > 2\omega_p^0$, it yields a region where the correlation dominates and provides negative GW corrections (the kink).

In conclusion, we presented an *ab initio* many-body GW calculation in graphene. The GW self-energy renormalizes by 17% the DFT Fermi velocity but does not open a gap at K. Close to the Dirac K point the linear band dispersion is considerably affected by correlation, leading to the appearance of a kink.

[1] K. S. Novoselov *et al.*, Nature (London) **438**, 197 (2005).
[2] Y. Zhang *et al.*, Nature (London) **438**, 201 (2005).
[3] C. Berger *et al.*, Science **312**, 1191 (2006).
[4] A. H. Castro Neto *et al.*, arXiv:0709.1163v1 [Rev. Mod. Phys. (to be published)].
[5] M. Calandra and F. Mauri, Phys. Rev. B **76**, 205411 (2007).
[6] A. Bostwick *et al.*, Nature Phys. **3**, 36 (2007).
[7] S. Y. Zhou *et al.*, Nature Mater. **6**, 770 (2007).
[8] S. Y. Zhou *et al.*, Physica (Amsterdam) **40E**, 2642 (2008).
[9] E. Rotenberg *et al.*, Nature Mater. **7**, 258 (2008).
[10] S. Y. Zhou *et al.*, Nature Mater. **7**, 259 (2008).
[11] S. Kim *et al.*, Phys. Rev. Lett. **100**, 176802 (2008).
[12] I. Brihuega *et al.*, Phys. Rev. Lett. **101**, 206802 (2008).
[13] C.-H. Park *et al.*, Phys. Rev. Lett. **99**, 086804 (2007).
[14] D. Prezzi *et al.*, Phys. Rev. B **77**, 041404(R) (2008).
[15] J. González, F. Guinea, and M. A. H. Vozmediano, Nucl. Phys. **B424**, 595 (1994); Phys. Rev. B **59**, R2474 (1999).
[16] S. Das Sarma, E. H. Hwang, and W.-K. Tse, Phys. Rev. B **75**, 121406(R) (2007); E. H. Hwang, B. Y.-K. Hu, and S. Das Sarma, Physica (Amsterdam) **40E**, 1653 (2008).
[17] E. G. Mishchenko, Phys. Rev. Lett. **98**, 216801 (2007).
[18] M. Polini *et al.*, Phys. Rev. B **77**, 081411 (2008).
[19] L. Hedin, Phys. Rev. **139**, A796 (1965); M. S. Hybertsen and S. G. Louie, Phys. Rev. Lett. **55**, 1418 (1985).
[20] R. W. Godby and R. J. Needs, Phys. Rev. Lett. **62**, 1169 (1989), and references therein.
[21] A. Fleszar and W. Hanke, Phys. Rev. B **56**, 10 228 (1997).
[22] See EPAPS Document No. E-PRLTAO-101-022849 for a more exhaustive description of our calculations. For more information on EPAPS, see http://www.aip.org/pubservs/epaps.html.
[23] T. Miyake and S. Saito, Phys. Rev. B **68**, 155424 (2003).
[24] C. Attaccalite *et al.*, arXiv:0808.0786.
[25] This GW result is stable over four different k meshes, increasing the convergence parameters and also moving to $k = 0.329$.
[26] T. Eberlein *et al.*, Phys. Rev. B **77**, 233406 (2008).
[27] C. Kramberger *et al.*, Phys. Rev. Lett. **100**, 196803 (2008).
[28] Hartree-Fock and Coulomb-hole plus screened-exchange approximation [19] calculations open the gap by 9 and 5 meV, respectively (34 and 13 meV at self-consistence, already achieved at the 2nd iteration), all below the typical $\sim \pm 0.1$ eV numerical error of *ab initio* calculations and so compatible with 0 band gap.
[29] K. Byczuk *et al.*, Nature Phys. **3**, 168 (2007).